Ferroptosis induction induced by ginkgetin enhances therapeutic effect of cisplatin in EGFR wild type non-small cell lung cancer

Jian-Shu Lou (jlouab@connect.ust.hk)
Hang zhou normal university
Li-Ping Zhao
Hang Zhou Normal University
Zhi-Hui Huang
Hang Zhou Normal University
Xia-Yin Chen
Hang Zhou Normal University
Jing-Ting Xu
The Hong Kong University of Science and technology
William Chi-Shing TAI
The Hong Kong polytechnic University
Karl W.K. Tsim
The Hong Kong University of Science and technology
Yi-Tao Chen
Zhejiang Chinese Medical University
Tian Xie
Hang Zhou Normal University

Research

Keywords: Ginkgetin, cisplatin, ferroptosis, non-small cell lung cancer, redox homeostasis

Posted Date: May 23rd, 2020

DOI: https://doi.org/10.21203/rs.3.rs-30027/v1

Abstract

Background Cisplatin (DDP) is the first-in-class drug for advanced and non-targetable non-small cell lung cancer (NSCLC). Recent study indicates that DDP could slightly induce non apoptotic cell death ferroptosis, and the cytotoxicity was promoted by ferroptosis inducer. The agents enhancing ferroptosis level therefore may increase anticancer effect of DDP. Several lines of evidence support the usage of phytochemicals in therapy of NSCLC. Ginkgetin, a bioflavonoid derived from *Ginkgo biloba* leaves, showed anti-cancer effect on NSCLC both *in vitro* and *in vivo*, which could strongly trigger autophagy. Ferroptosis can be triggered by autophagy, and which regulates redox homeostasis. Thus, we aim to elucidate the possible role of ferroptosis induction in accounting for synergy of ginkgetin with DDP in cancer therapy.

Methods Ginkgetin promoted DDP-induced anticancer effect was observed via cytotoxicity assay and western blot. Ferroptosis triggered by ginkgetin in DDP treated NSCLC was observed via lipid peroxidation assay, labile iron pool assay, western blot, and QPCR. With ferroptosis blocking, the contribution of ferroptosis on ginkgetin + DDP induced cytotoxicity, Nrf2/HO-1 axis and apoptosis were determined via luciferase assay, immunostaining, chromatin immunoprecipitation (CHIP), and flow cytometry. The role of ferroptosis in ginkgetin + DDP treated NSCLC cells was illustrated by the application of ferroptosis inhibitor, which was further demonstrated in xenograft nude mice model.

Results Ginkgetin synergized cisplatin in cytotoxicity in NSCLC cells, which concomitant with increased labile iron pool and lipid peroxidation: both these processes were the key characteristics of ferroptosis. The induction of ferroptosis, mediated by ginkgetin, was further confirmed by decline expressions of SLC7A11, GPX4 and GSH/GSSG ratio. In parallel, ginkgetin disrupted redox hemeostasis in DDP-treated cells, demonstrated by the enhanced ROS formation and inactivation on Nrf2/HO-1 axis. Ginkgetin also enhanced DDP-induced mitochondrial membrane potential (MMP) loss and apoptosis in cultured NSCLC cells. Furthermore, blocking ferroptosis reversed the gingketin-induced inactivation on Nrf2/HO-1, as well as the elevation on ROS formation, MMP loss and apoptosis in DDP-treated NSCLC cells.

Conclusion This study firstly reported that ginkgetin promoted DDP-induced anticancer effect, which could be accounted by induction of ferroptosis.

Background

Lung cancer is the leading cause of cancer-related death throughout the word. The global incidents of lung cancer ranked first in 2018 among all types of cancer[1]. The mortality and incidents are climbing up quickly in recent years. In china, the mortality and incidents were much higher than other regions[2], the mortality is expecting to increase by ~ 40% during 2015–2030[1]. Non-small lung cancer (NSCLC) is the most common type of lung cancer, which account for more than 80% of total lung cancers. For NSCLC treatment, immunotherapy usually have low response rate. While target therapy is highly dependent on oncogenic mutation, which accounts for small percentage of total NSCLC. Thus, cisplatin (DDP), a

platinum-based chemotherapeutic drug, is still a standard treatment for non-targetable NSCLC, especially for EGFR wild type NSCLC patients, as well as the patients in advanced stage. Combined drug therapy is a promising strategy to treat NSCLC, especial for those classic chemo-therapeutic drugs. DDP usually combined with other chemo-drugs in treating NSCLC. However, patients with advanced stage of cancer, or poor overall health, might not tolerate the unexpected side effects, as induced by combination of chemo-drugs[3]. Therefore, the focus has shifted to a combination of phytochemicals with DDP, as to increase the therapeutic effect or to eliminate side-effects. Extensive studies demonstrated that phytochemicals could enhance the sensitivity of DDP without overlapping toxicity[4]. The DDP resistance is resulted from increase of apoptosis resistance and redox homeostasis resetting: these are two key processes involving therapeutic efficacy of DDP. Thus, phytochemicals trigger non-apoptotic cell death or disrupt the redox homeostasis resetting could be effective in enhancing chemosensitivity of DDP, as well as in preventing emergence of resistance.

Ferroptosis is a mode of non-apoptotic cell death, which triggers cell death via iron-dependent lipid peroxidation[5]. Recent study demonstrated that ferroptosis is a novel anticancer action for DDP[6]. Erastin, a classic ferroptosis inducer, induces ferroptosis via system Xc^- inhibition, and which has been shown to synergize with DDP in promoting cytotoxicity in different types of tumor, especially in NSCLC[6–8]. The drug resistance to DDP occurs via apoptotic evasion, and therefore ferroptosis is being considered as a new therapeutic way in promoting the efficacy of DDP.

The heart of ferroptosis is lipid peroxidation and iron accumulation. Ferroptosis is driven by lipid peroxidation, which typically triggers via suppression on solute carrier family 7 member 11 (SLC7A11) and glutathione peroxidase 4 (GPX4). SLC7A11 is a cystine-glutamate anti-porter. The reduction of SLC7A11 expression leads to cystine depletion, glutathione (GSH) shortage and consequent lipid peroxidation elevation[9]. GPX4, a key inhibitor on lipid-peroxidation, oxidizes GSH to glutathione disulfide (GSSG). Repressing GPX4 compromised the capability in neutralizing lipid peroxidation via GSH[10]. In balancing iron, transferrin and Solute Carrier Family 40 Member 1 (SLC40A1) are crucial to maintain intracellular iron concentration. Transferrin imports iron into cells; while SLC40A1 exports iron from cells[11]. Thus, the increase on transferrin and decrease on SLC40A1 could cause intracellular iron accumulation. Cancer cells are usually adapting to iron and under persistent oxidative stress. To protect from ferroptosis-induced cell death, cancer cells can promote their antioxidant systems[5]. For instance, nuclear factor erythroid 2–related factor 2 (Nrf2), a master antioxidant regulatory transcription factor, prevents ferroptosis-induced cell death via upregulating antioxidant enzymes[12]. For instance, heme oxygenase-1 (HO-1), a key antioxidant enzyme, contains multiple number of antioxidant response element (ARE) on its promoter region[13]. In line to this notion, cancer cell having mutations in Nrf2 is able to increase transcription of antioxidant genes. The induction of ferroptosis through SLC7A11 and GPX4 could be mitigated via Nrf2/HO-1 activation via lipid oxidation elimination. Therefore, phytochemicals having suppression of Nrf2/HO-1 antioxidant system could be effective in promoting ferroptosis.

Ginkgetin, a bioflavonoid derived from *Ginkgo biloba* leaves, has been proposed in treating colorectal[14], lung[15] and breast cancer[16]. By drug screening platform, ginkgetin was identified to have better synergistic effect with DDP in inducing cytotoxicity on NSCLC. We previously reported that ginkgetin induced autophagy, and apoptosis inhibitors could not reverse ginkgetin induced cytotoxicity[15]. Considering autophagy induction has been proposed to degrade key factors of ferroptosis in cancer cells, which thereafter could trigger ferroptosis[17,18]. Thus, it is intriguingly to elucidate the possible role of ferroptosis induction in accounting for ginkgetin-induced promotion on anticancer effect of DDP in NSCLC.

Materials And Methods

Cell lines, reagents and antibodies

A549 cell line was obtained from the American Tissue and Cell Collection (ATCC, Manassas, VA). NCI-H460 and SPC-A-1 cell lines were kindly gifted by Dr. William Dai in The Hong Kong Polytechnic University. Ginkgetin (>98% purity) was obtained from Chengdu Must Bio-technology Ltd. (Chengdu, China). Annexin V-FITC Apoptosis Detection Kit was purchased from BD Biosciences (San Jose, CA). fumarate, sulforaphane, desferoxamine and deferiprone were purchased from MedChemExpress (Monmouth Junction, NJ). Cisplatin (DDP), 5,5',6,6'-tetrachloro-1,1',3,3'-tetraethyl-imidacarbocyanine iodide (JC-1) and 2',7'-dichlorofluorescin diacetate (DCFH-DA) were obtained from Sigma-Aldrich (St. Louis, MO). Calcein-acetoxymethyl ester (CA-AM) was purchased from Shanghai Yisheng Biotechnology Co. (Shanghai, China). BODIPY™ 581/591 C11 was obtained from Thermo Fisher Scientific (Waltham, MA). The culture medium and FBS was obtained from Invitrogen Technologies (Carlsbad, CA). The plasmid pARE-Luc was obtained from Promega Corporation (Madison, WI). The antibodies were obtained from the following sources: Nrf2, HO-1, GPX4, and transferrin were purchased from Abcam (Cambridge, UK); α-tubulin from Sigma-Aldrich (St. Louis, MO); cleaved-PARP, cleaved-caspase 3, cleaved-caspase 7, cleaved-caspase 9, SLC7A11, SLC40A1, horseradish peroxidase (HRP)-conjugated goat anti-rabbit antibody, HRP-conjugated goat anti-mouse antibody and Alexa Fluor 555-conjugated goat anti-rabbit antibody were from Cell Signalling Technology (Danvers, MA).

Cell viability assay

Cell viability assay was conducted as previously described[19]. In brief, cells were seeded in 96-well plates, after drug treatment, MTT reagent was added (5 mg/μL, 20 μL/well), incubation for 4 hours. After removing the medium, formazan was dissolved in DMSO (200 μL/well), shacking for 15 min, before the reading by spectrophotometric absorbance at 570 nm.

Apoptosis detection

Cells were treated with ginkgetin, DDP and ginkgetin + DDP. The apoptosis rates of untreated and treated cells were detected by Annexin V-FITC Apoptosis Detection Kit, as previously described[19]. Both floating and adherent cells were collected and wash 3 times by PBS. Cells were stained with Annexin V and PI for 15 min in dark, and detected apoptosis via flow cytometry with the acquisition criteria of 10,000 events for each sample.

Total ROS and MMP measurement

The measurement of total ROS and MMP were conducted as previously described[20]. For total ROS detection, 15 μM DCFH-DA was added in culture medium without FBS for 0.5 hour. After washing cells twice with PBS, cells were collected and analyzed by flow cytometry (Exc=488 nm, Em=530 ± 30). For MMP measurement, cells were stained with JC-1 for 30 min, then washed twice with PBS before analysis. Both JC-1 monomers (Exc=488 nm, Em=530 ± 30) and aggregates were detected (Exc=561 nm, Em=582 ± 25). Each sample met the acquisition criteria of 10,000 events, and the results were analyzed with Flowjo v7.6 software.

Lipid peroxidation measurement

C11-BODIPY (10 μM) was added to drug treated and untreated cells for 0.5 hour, then cells were collected by trypsin. Oxidation of the polyunsaturated butadienyl portion of C11-BODIPY resulted in a shift of the fluorescence emission peak from ~590 nm to ~510 nm. Cells were analyzed using flow cytometry (Exc=488 nm, Em=510) after washing twice with PBS, and the results were analyzed with Flowjo v7.6 software.

Measurement of labile iron pool (LIP)

Drug treated and untreated cells were collected and washed 2 times with PBS. Then, cells were loaded with CA-AM (0.25 μM) at the density of 0.5×10^6/ml for 15 min. After washing twice with PBS, cells were incubated with iron chelator deferiprone (100 μM) for 1 hour or untreated. Measurement was conducted using fluorescence microplate reader (Exc=488 nm, Em=525). The amount of LIP was reflected via difference on mean fluorescence of each sample with or without deferiprone.

RNA isolation and real-time PCR

RNAzol RT reagent was used to extract total RNAs, which reversed into cDNAs using HiScript®II One Step qRT-PCR Kit (Vazyme, Shanghai, China) according to the manufacturer's instruction. In brief, collected cells were lysed with RNAzol RT reagent. RNA was separated by adding RNase-free ddH_2O to lysate, after centrifuging, the aqueous layer was collected. RNA was precipitated and washed by ethanol. After removing ethanol, RNA was dried and re-suspended in RNase-free ddH_2O. The concentration of RNA was

quantified by spectrometry. Next, 1 μg RNA was diluted to 12 μL by RNase-free ddH_2O, and 4 μL 4 × gDNA wiper Mix was added, mixed and incubated at 42 ^oC for 2 min. After adding 4 μL 5 × HiScript III qRT SuperMix, reverse transcription was conducted at 37 ^oC for 15 min, and stopped at 85 ℃ for 5 sec. The following primers were used: 5′-CCA GGC AGA GAA TGC TGA GTT C-3′ (S) and 5′-AAG ACT GGG CTC TCC TTG TTG C-3′ (AS) for HO-1; 5′-TCC TGC TTT GGC TCC ATG AAC G-3′ (S) and 5′-AGA GGA GTG TGC TTG CGG ACA T-3′ (AS) for SLC7A11; 5′-ACA AGA ACG GCT GCG TGG TGA A-3′ (S) and 5′-GCC ACA CAC TTG TGG AGC TAG A-3′ (AS) for GPX4; 5′-GAG ACA AGT CCT GAA TCT GTG CC-3′ (S) and 5′-TTC TTG CAG CAA CTG TGT CAC AG-3′ (AS) for SLC40A1; and 5′-AAC GGA TTT GGC CGT ATT GG-3′ (S) and 5′-CTT CCC GTT CAG CTC TGG G-3′ (AS) for GAPDH. Real-time PCR was performed using SYBR Green Master mix (Vazyme) by Bio-Rad qPCR system (Bio-Rad, Hercules, CA). The data were normalized to amount of GAPDH housekeeping genes.

Western blot analysis

Western blot was conducted as described[20]. Briefly, cells were lysed, and their protein concentrations were measured using Bradford method. SDS-PAGE was used to separate the protein in each sample. Proteins were transferred from gel to membrane. Then, the membrane was blocked and incubated with indicated primary antibodies. The blots were rinsed before probed with secondary antibodies. The reactive bands were visualized by ECL and calibrated by Chemidoc Imaging System (Bio-Rad).

Immunofluorescence

Cultured A549 cells were seeded on coverslips. Ginkgetin, DDP and ginkgetin + DDP were added for 48 hours. Cells were fixed with 4% formaldehyde after rinsing twice with PBS. Specimens were blocked (1X PBS/5% BSA/0.3% Triton™ X-100) for 1 hour. Then, primary antibody was incubated overnight at 4°C. Then, cells were rinsed 3 times, and probed with Alexa Fluor 555-conjugated goat anti-rabbit secondary antibody for 2 hours. After rinsing, coverslips were mounted to slide by Prolong® Gold Antifade Reagent with DAPI (CST, Danvers, MA). Images were taken by FV3000 Confocal Laser Scanning (Olympus, Japan). To analyse nuclear translocation of HO-1, the co-localization coefficients were calculated using Olympus Fluoview FV31S-DT Software.

Chromatin immunoprecipitation

Chromatin immunoprecipitation was performed using ChIP kit (Abcam, Cambridge, UK). In brief, the proteins were cross-linked to DNA by formaldehyde for 15 min at room temperature. Glycine was added to quench the formaldehyde at final concentration of 125 mM. Cells were washed by ice-cold PBS for 3 times, then resuspended in lysis buffer. The cross-linked lysate was sonicated to shear DNA to an average

fragment size of 200-800 bp, then centrifuged and transferred the supernatant for immunoprecipitation. The sonicated chromatin (100 μg) was incubated with anti-Nrf2 antibody, or IgG, or H3 antibody overnight at 4 °C with rotation. DNA purification was carried out according to the manufacturer's instructions. Then, HO-1 DNA was amplified for 45 cycles of PCR with the following primers: 5'- TCA ATA GGC GAT CAG CAA GGG -3' (S) and 5'- TGG AAT GCG TGG GAC ACT C -3' (AS).

Luciferase assay

Luciferase assay was conducted as previously described[20]. In brief, drug treated and untreated cells were washed and lysed. The supernatant was collected and then analysed using a commercial kit (Thermo Fisher Scientific).

Amino acids detection

Culture A549 cells were treated with ginkgetin, DDP and ginkgetin + DDP for 48 hours. Then, cultured cells at least 10^7 cells for each group was collected. Two hundred μL precipitant (methanol: acetone: water = 2:2:1) was added to each sample, followed by sonication at 4 ^{o}C for 10 min. Samples were stayed at -20 ^{o}C for 2 hours. Then, the supernatant was lyophilized, and resolved in 160 μL methanol. The levels of glutamate and cystine were detected by Sciex 5500 LC-MS/MS. Data were analysed by MultiQuant software (SCIEX, Framingham, MA)

GSH/GSSG assay

Cultured A549 cells were treated with ginkgetin, DDP and ginkgetin + DDP for 48 hours. The intracellular level of GSH and GSSG were performed by GSH and GSSG Assay Kit (Beyotime, Shanghai, China), according to the protocol given by manufacturer. Briefly, cells were collected and lysed, then centrifuged at 10,000 × g for 10 min. The supernatant was mixed with GSH assay buffer, GSH reductase, 5,5'-dithio-bis 2-nitrobenzoic acid solution and incubated at 25 °C for 5 min, then NADPH was added. The absorbance at 412 nm was measured by microplate reader. The concentration of total glutathione, or GSSG, was calculated via standard curve, and GSH level was calculated as: GSH = (total glutathione-GSSG) × 2. The ratio of GSH/GSSG was calculated as [GSH]/[GSSG].

Xenograft nude mice model

The establishment of xenograft nude mouse model and ginkgetin preparation were conducted as previously described[15]. Briefly, when tumours on transplanted nude mice reached around 100 mm^3, the mice were randomized divided into eight groups: control, ginkgetin, DDP, ginkgetin + DDP, UAMC 3203, ginkgetin + UAMC 3203, DDP + UAMC 3203, ginkgetin + DDP + UAMC 3203. Both DDP (3 mg/kg) and ginkgetin (30 mg/kg) were administered by intraperitoneal injection, with 2 - 3 times per week and once per day, respectively. UAMC 3203 (10 mg/kg) was administered 5 days/week by intraperitoneally injection. Tumour size and body weight were measured 3 times per week. After dosing 31 days, the nude mice were sacrificed, and tumours were removed and weighed. Animal experiments were performed in accordance with National Institutes of Health Guide for Care and Use of Laboratory Animals, approved by Hangzhou Hibio Experimental Animal Ethics Committee (Permit Number: HB201510024-B).

Statistical analysis

Statistical analysis conducted by using one-way analysis of variance. Statistically significant changes were classified as significant (*) where $p < 0.05$, more significant (**) where $p < 0.01$ and highly significant (***) where $p < 0.001$, as compared with control or indicated group.

Results

Ginkgetin promotes DDP-induced cytotoxicity

Ginkgetin, a biflavonoid from *Ginkgo biloba* leaves, exhibited cytotoxicity in cultured A549 cells[15]. Here, ginkgetin was combined with DDP at various concentrations in applying onto cultured A549 cells. Majority of combinations (ginkgetin + DDP) significantly increased the cytotoxicity, as compared with single usage of DDP or ginkgetin (Fig. 1A). The combination index indicated that ginkgetin at 5 μM, together with different concentrations of DDP, showed the lower CI value, suggesting a better synergy (Fig. 1B). The synergistic effect of GK at 5 μM with DDP were also demonstrated in NCI-H460 and SPC-A-1 NSCLC cells (Fig. S1A&B). All these three NSCLC lines are EGFR wild type, which are not sensitive to target therapy, but more suitable for DDP treatment. Among these combinations, the mixture of ginkgetin and DDP (both at 5 μM) showed the relative lower CI value, and the lowest CI value at 0.5005 was observed in A549 cell line (Fig. 1B&C, S1B). To reveal pharmacodynamic interaction of ginkgetin and DDP on A549, a response surface fitting was constructed. As expected, the combination of ginkgetin and DDP, both at 5 μM each, was located on the highest region of dose–response surface, further confirmed that this combination having better anti-cancer function (Fig. 1D). This combination ratio was chosen for further mechanistic study.

Ginkgetin induces ferroptosis in DDP-treated cells

Previous study demonstrated ginkgetin induces autophagic cell death[15], However, this phenomenon was not further promoted in ginkgetin + DDP treated cells. As ferroptosis is considered to be a consequent

event after autophagy in recent year[17,18]. Thus, we hypothesis ferroptosis might be triggered in this combination. The two key characteristics of ferroptosis are lipid peroxidation and intracellular-free iron[21]. C11-BODIPY$^{581/591}$ could be used as a lipid peroxidation probe in mammalian cells[22]. Free iron levels could be measured via labile iron pool (LIP), stained by CA-AM[17]. Thus, C11-BODIPY$^{581/591}$ and CA-AM were employed here to observe lipid peroxidation and LIP, respectively. DDP did not alter the levels of lipid peroxidation and LIP in A549 cells; while ginkgetin significantly increased the levels to~2.6 and ~2.4 folds respectively (Fig. 2A&B). The combination of ginkgetin + DDP further increased the levels of lipid peroxidation and LIP to ~3.3 and ~7.1 folds, respectively (Fig. 2A&B). The enhancement of LIP was more robust than that of lipid peroxidation in ginkgetin + DDP-treated cells. Ginkgetin induced promotion on lipid peroxidation and LIP were also observed in DDP-treated NCI-H460 and SPC-A-1 cells (Fig. S2A&B).

SLC7A11 and GPX4 are main targets for ferroptosis induction. Thus, we revealed expressions of SLC7A11 and GPX4 at transcriptional and post-transcriptional level after the treatment of combined drugs. There were no significant changes on SLC7A11 and GPX4 mRNAs after the combined drug treatment in cultured A549 cells (Fig. 2C). In contrast to mRNA level, the protein amounts of SLC7A11 and GPX4 were markedly decreased in application of ginkgetin + DDP in A549, NCI-H460 and SPC-A-1 cells (Fig. 2D, S2C). These phenomena suggested the role of ginkgetin in increasing protein degradation of SLC7A11 and GPX4 in DDP-treated NSCLC cells. To further demonstrate the ferroptosis induction, we determined another key factor involving in iron accumulation during ferroptosis, i.e. SLC40A1 and transferrin. SLC40A1 is the sole iron exporter in mammalian cells, as well as a downstream target of Nrf2[23]; while transferrin imports iron to cell[24]. In the cultures, DDP sharply increased the mRNA and protein levels of SLC40A1 (Fig. 2E&D). Gingketin alone did not change the mRNA level of SLC40A1; however, which could reverse the DDP-induced elevation on mRNA (Fig. 2E), as well as protein level (Fig. 2D). For the case of transferrin, DDP slightly increased the protein amount in A549 cells (Fig. 2D), while have no obvious change on NCI-H460 and SPC-A-1 cells (Fig. S2C). Ginkgetin combine with DDP sharply increased transferrin expression in all these three NSCLC cells (Fig. 2D, S2C). The decreased SLC40A1 and increased transferrin might account for LIP elevation in combination treatment.

The inhibition on SLC7A11 triggers ferroptosis via cystine/glutamate transport. The reduction of SLC7A11 is expected to decrease glutamate release and cystine uptake. In accordance with this notion, we measured the levels of cystine and glutamate in drug treated A549 cells. The intracellular cystine was significantly decreased, accompanied with notably increased glutamate level, after the treatment of ginkgetin (Fig. 2F). No significant change of glutamate was observed in DDP-treated cells; while the cystine level was notably increased, which might contribute to the increased antioxidant activity. The combined treatment sharply reversed DDP-induced elevation on cystine, and significantly increased glutamate level, as compared to control (Fig. 2F). These results indicated that the anti-porter function of SLC7A11 was partially reversed after application of ginkgetin in DDP-treated A549 cells.

GSH is synthesized from cystine and eliminates lipid ROS via GPX4. As the decline of cystine and GPX4 were observed here after the combined drug treatment, thus the intracellular GSH level was determined. As expected, GSH amount was significantly decreased by ginkgetin. However, the GSH amount was increased after application of DDP, which might be due to the redox resetting via antioxidant system. The combined drug treatment sharply reversed DDP-induced increase on GSH (Fig. 2G). GSH is highly reactive with lipid ROS to generate glutathione disulfide (GSSG), and the reduced ratio of GSH/GSSG is considered to be a marker of oxidative stress. Ginkgetin + DDP application sharply decreased the ratio of GSH/GSSG (Fig. 2H), indicating elevation of oxidative stress. All these data illustrated above indicated that ferroptosis was being triggered in the drug combination.

Ginkgetin downregulates Nrf2/HO-1 axis in DDP-treated NSCLC cells

Ferroptosis could be downregulated by famous antioxidant system Nrf2/HO-1 via neutralized on oxidative stress, which responsible for the compromised anticancer function of DDP[25,26]. Our previous study has demonstrated ginkgetin could reduce Nrf2 activation, thus we hypothesis that it could downregulate elevated activity on Nrf2/HO-1 axis induced by DDP. Here, neither ginkgetin nor DDP could change the expression of Nrf2, which however was sharply reduced in treatment of ginkgetin + DDP in A549, NCI-H460 and SPC-A-1 cells (Fig. 3A, S3A&B). DDP slightly increased the expression of HO-1 in A549 cells (Fig. 3A), there are no significant change in NCI-H460 and SPC-A-1 cells (Fig. S3A&B); while ginkgetin robustly deceased the amount of HO-1 in all these three NSCLC cells (Fig. 3A, S3A&B). Activated Nrf2 binds to ARE and upregulates transcription of HO-1. To detect the effect of ginkgetin + DDP on ARE-mediated transcriptional activity, a luciferase reporter pARE-Luc was applied. This construct contained four repeats of antioxidant response element (ARE) and a luciferase reporter gene luc2P. In pARE-Luc-expressed A549 cells, DDP activated ARE-mediated transcription by ~3 folds; while ginkgetin did not show activation on ARE-mediated transcription (Fig. 3B). Application of ginkgetin in DDP-treated A549 cells largely reversed DDP-induced activation on ARE-mediated transcription, i.e. counter acting the induction by DDP (Fig. 3B). CHIP assay was applied to identify the binding of Nrf2 to HO-1 promoter. DDP sharply increased the binding of Nrf2 to HO-1 promotor by over 40 folds (Fig. 3C). Ginkgetin alone showed no significant change on this binding. As expected, ginkgetin sharply reduced DDP-induced elevation on the binding of Nrf2 to HO-1 promoter (Fig. 3C). Binding of Nrf2 to HO-1 promoter is leading to transcription of HO-1. In cultured A549 cells, DDP increased the mRNA expression of HO-1 (Fig. 3D). The application of ginkgetin significantly reversed DDP-induced upregulation of HO-1 mRNA expression (Fig. 3D). In consistent, this mRNA regulation was in line to protein level, ginkgetin reversed the DDP-induced HO-1 protein expression (Fig. 3A). These results indicated that DDP could promote the antioxidant system Nrf2/HO-1 to cope with ferroptosis induced oxidative stress, which could be reversed by ginkgetin.

The antioxidant activity, induced by Nrf2, is further enhanced by nuclear translocation of HO-1[27]. Thus, the change on HO-1 nuclear translocation in ginkgetin, DDP and ginkgetin + DDP-treated A549 cells was revealed by immunostaining. The fluorescence intensity of HO-1 was observed both in cytosol and nucleus. In control group, the fluorescence was mainly located in cytosol, and a faint signal was observed in nucleus, as demonstrated by co-localization of DAPI signal. Application of DDP notably increased the HO-1 fluorescence intensity in nucleus; however, ginkgetin decreased significantly nuclear expression of HO-1 and sharply reversed DDP-induced HO-1 nuclear translocation (Fig. 3E&F). This result further confirmed that ginkgetin could reverse DDP-induced activation on Nrf2/HO-1 axis, which contribute to the mitigation on antioxidant effect in ginkgetin + DDP treated NSCLC cells.

Ferroptosis inhibition reversed ginkgetin induced promotion on cytotoxicity of DDP

To further observe the role of ferroptosis in ginkgetin + DDP induced anticancer function. Ferroptosis inhibitors UAMC 3203 and DFO were applied. Here, both UAMC 3203 and DFO markedly reversed ginkgetin + DDP induced cytotoxicity in cultured A549, NCI-H460 and SPC-A-1 NSCLC cells (Fig. 4A, S4A&B). However, the Nrf2 activators DMF and SFN could not reverse ginkgetin + DDP induced cytotoxicity in all three NSCLC cells (Fig. 4B, S4A&B). The upregulation of DMF and SFN on Nrf2 was demonstrated by western blot, that the amount of Nrf2 were significantly increased by DMF and SFN in ginkgetin + DDP treated A549 cells (Fig.S4C). These phenomena indicated that the Nrf2 is not the nodal for ginkgetin + DDP induced cytotoxicity.

UAMC 3203 is a novel ferroptosis inhibitor. The reverse effect of UAMC 3203 in ginkgetin + DDP induced cytotoxicity was much obvious than DFO (Fig. 4A, S4A&B), which might be due to its better activity on ferroptosis suppression. Thus, we use UAMC 3203 for further observation. To confirm the ferroptosis suppression, the key markers lipid peroxidation, LIP, SLC7A11 and GPX4, were determined in A549 cultures. The application of UAMC 3203 moderately reversed ginkgetin-induced elevation on lipid peroxidation (Fig. 4C&D) and LIP (Fig. 4F), and this effect was much obvious in the scenario of ginkgetin + DDP (Fig. 4C, D&F). In parallel, UAMC 3203 reversed gingketin + DDP mediated decline of SLC7A11; while the reverse effect on GPX4 was identified in cultures being treated with gingketin or gingketin + DDP (Fig. 4E). These results indicated that ferroptosis, induced by ginkgetin + DDP, was blocked by UAMC 3203.

Considering ferroptosis induction could directly or indirectly downregulated GPX4, leading lipid peroxidation. To confirm the role of ferroptosis in ginkgetin + DDP induced cytotoxicity. We overexpressed GPX4 in A549 cells, the upregulated expression of GPX4 was confirmed by western blot in ginkgetin + DDP treated cells (Fig. 4G). To our respective, the cytotoxicity was notably decreased after GPX4 overexpression (Fig. 4H), concomitant with the downregulation on lipid peroxidation (Fig. 4I), and LIP

(Fig. 4J). This result further elucidated that ferroptosis contributes to ginkgetin + DDP induced cytotoxicity.

Ferroptosis suppression mitigated attenuation on Nrf2/HO-1 activation and ROS promotion induced by ginkgetin

Redox homeostasis is governed by the balance of antioxidant system and ROS formation. The downregulation on antioxidant system Nrf2/HO-1 induced by ginkgetin in DDP treated NSCLC has driven us to found if ROS was further increased to disrupt the redox homeostasis. In cultured NSCLC cells, DDP-induced ROS formation, and which was sharply promoted by ginkgetin in A549, NCI-H460 and SPC-A-1 cells (Fig. 5A&B, S5A). However, blocking ROS formation via N-acetylcysteine failed to reverse ginkgetin + DDP induced cytotoxicity (Fig. S5B).

Since ferroptosis inhibitors, not Nrf2 activators, could largely reversed ginkgetin + DDP induced cytotoxicity. In addition, the unchanged mRNA level of SCL7A11 and GPX4 partial indicated that these two ferroptosis genes were not transcriptionally regulated by Nrf2. Thus, we hypothesis that Nrf2/HO-1 antioxidant inactivation and ROS enhancement could be a consequent event of ferroptosis. Here, application of UAMC 3203 sharply rescued gingketin + DDP induced decline of Nrf2 (Fig. 5C), as well as ARE-mediated transcription activity (Fig. 5D). In addition, UAMC 3203 application reversed the ginkgetin + DDP suppressed expressions of mRNA and protein of HO-1 (Fig. 5G&C). Consistent with this, ginkgetin + DDP induced ROS increasement was sharply reversed by the application of UAMC 3203 in A549, NCI-H460 and SPC-A-1 cells (Fig. 5H, S5C). These results indicated that ferroptosis suppression mitigated attenuation on Nrf2/HO-1 activation and promotion on ROS formation induced by ginkgetin in DDP treated NSCLC cells.

Ginkgetin promoted DDP-induced apoptosis was alleviated via ferroptosis suppression

ROS elevation induced by ginkgetin in DDP-treated cells might result in increasing cell sensitivity to ROS. One consequent event of ROS elevation is the loss of mitochondria membrane potential (MMP). Here, we demonstrated that ginkgetin notably increased the MMP loss in DDP-treated A549 cells (Fig. 5E&F). MMP loss could lead to activation on caspase-9, consequently activate caspase-3, -7, leading apoptosis. As apoptosis is the key mechanism for DDP-induced anticancer effect. Thus, we observed if apoptosis was increased after ferroptosis induction. Here, we found that DDP at 5 μM slightly increased the apoptosis rate at ~15%: while ginkgetin at 5 μM induced apoptosis at ~30% (Fig. 6A&B). The combined DDP and ginkgetin sharply increased the apoptosis rate to over 50%, which was confirmed by increased apoptotic markers, i.e. cleaved-caspase 3, cleaved-caspase 7 and cleaved caspase 9, as revealed by western blotting (Fig. 6C&D).

Intriguingly, blocking apoptosis via Q-VD-Oph could statistically significantly reversed DDP-induced apoptosis, but could not reverse ginkgetin induced promotion on DDP-induced cytotoxicity (Fig. 6E). While ferroptosis suppression significantly reversed apoptosis in ginkgetin+DDP treated cells (Fig. 6F). Consistent with this, ferroptosis suppression attenuated ginkgetin + DDP induced MMP loss (Fig. 5I), characterized with the sharply increase on the mean FITC fluorescence and decline on PerCP-Cy5-5 fluorescence (Fig. 5J), which indicated the reduced MMP loss. These results indicated that ferroptosis might contribute to ginkgetin induced promotion on DDP triggered apoptosis.

Ginkgetin enhanced anticancer effect of DDP is compromised by ferroptosis suppression in xenograft nude mice model

To further confirm the ginkgetin induced promotion on anticancer function of DDP, we applied A549 xenograft nude mice model. After the treatment of 31 days, the mean body weight of DDP treated group significantly declined; while ginkgetin group showed no significant change, as compared with control mice (Fig. 7A). Combined administration of ginkgetin + DDP significantly increased the mean body weight since day 25, as compared with DDP group (Fig. 7A), which might indicate that ginkgetin treatment could relieve DDP-induced toxicity. The mean tumor volumes in DDP, ginkgetin, and ginkgetin + DDP group were decreased: the best reduction was revealed in the combined administration group (Fig. 7B). When combined with UAMC 3203 administration, the mean tumor volume was not statistically significantly changed in control group, as well as in DDP group. Ginkgetin group showed moderately increase on mean tumor volume in the presence of UAMC 3203. However, a notably increase was identified in ginkgetin + DDP group after UAMC 3203 treatment (Fig. 7B). Consistent with the change on tumor volume, the mean tumor weight was smallest in ginkgetin + DDP group (Fig. 7C&D). UAMC treatment statistically significantly reversed the tumor shrink in ginkgetin group, however, the reversed effect was more robustly in ginkgetin + DDP group (Fig. 7C&D).These results consistent with *in vitro* study in supporting the notion that ginkgetin induced promotion on anticancer effect of DDP in NSCLC could be mediated by ferroptosis.

Discussion

DDP combines with phytochemicals is a promising strategy to enhance its anticancer effect in NSCLC. In this study, we revealed the synergistic effect of gingketin with DDP on cytotoxicity in EGFR wild type NSCLC. The synergy of combined drugs was further confirmed in animal study. Apoptosis resistance and redox resetting are key factors in accounting for failure of DDP therapy, and therefore the strategy in triggering non-apoptotic cell death and disruption on redox balance could be promising methods to enhance anticancer function of DDP. Here, ferroptosis, a non-apoptotic cell death, was robustly triggered by gingketin application in DDP treated EGFR wild type NSCLC cells, concomitant by inactivation on Nrf2/HO-1 axis and promotion on total ROS formation. In addition, DDP-induced MMP loss and apoptosis were robustly amplified under ginkgetin application. Furthermore, the suppression on ferroptosis could diminish the synergy of gingketin + DDP, as well as reverse the inactivation on Nrf2/HO-1, ROS enhancement, MMP loss and apoptosis. This is the first time to demonstrate that ferroptosis

could account for increased therapeutic effect of DDP induced by ginkgetin both *in vitro* and *in vivo* systems.

Ferroptosis is dependent on iron and characterized by lipid peroxidation, which could ultimately cause oxidative cell death[28]. Recent report has suggested that autophagy could trigger ferroptosis, and some of them believed that ferroptosis is a part of autophagy process[5]. In line to this notion, ginkgetin, which robustly triggers autophagy, could has potential effect on ferroptosis induction.

Ferroptosis induced by direct or directly suppression on GPX4 to decline GSH-medicated antioxidant activity, contributing to elevation on lipid peroxidation. GPX4 is a selenoenzyme, catalyzing GSH to GSSG, as to neutralize production of lipid peroxidation. As GPX4 is the most functional selenoenzymes in reducing esterified lipid hydroperoxide, its reduction notably increases lipid peroxidation[29]. SLC7A11 is a cystine/glutamate antiporter. Suppression on SLC7A11 could induce autophagy via activation on lysosomal-associated membrane protein 2a, which in turn degrades GPX4[30]. In addition, SLC7A11 inactivation leads to reduced intracellular concentration of cystine and increased the glutamate level. Cystine is an essential substrate for GSH synthesis; while the reduction of cystine leads to decline of GSH. This could disrupt the equilibrium of antioxidant system and thereafter enhance lipid peroxidation[31,32]. Consistent with this theory, expression of SLC7A11 and GPX4 expression, GSH level, and GSH/GSSG ratio, were sharply decreased, which might contribute to robustly increase on lipid peroxidation in combined drug treatment. Furthermore, SLC40A1 and transferrin contribute to export and import of iron, respectively. The decreased SLC40A1 and increased transferrin were observed here, which contributed to elevation of LIP (Fig. 8). Thus, the phenomena illustrated here indicated that ferroptosis was triggered by gingketin + DDP application.

The crucial role of ferroptosis on anticancer effect of ginkgetin + DDP combination was further demonstrated by the ferroptosis inhibition. Blocking ferroptosis significantly reverse ginkgetin + DDP induced anticancer effect both in vitro and in vivo. Intriguingly, the ferroptosis key factors SLC7A11, GPX4, and SLC40A1 are all transcriptionally regulated by Nrf2. However, only the mRNA expression of SLC40A1 was significantly changed. In addition, ferroptosis blocking could largely reverse Ginkgetin + DDP induced decrease on Nrf2. The inhibition on Nrf2 could not significantly rescued ginkgetin + DDP induced cytotoxicity. These phenomena might be due to the promoted degradation on SLC7A11 and GPX4, which evoked ferroptosis, consequently downregulated Nrf2 mediated suppression on SLC40A1, finally increase the transcriptional and post-transcriptional level of SLC40A1. Our previously study has demonstrated that ginkgetin induces autophagy via p62. The decline of p62 could downregulate Nrf2, we do find the decline on p62 in drug combination (Fig. S6), however, the detailed mechanism needs to be further studied.

Nrf2 is a master regular on antioxidant and detoxification, which is responsible for ferroptosis resistance via binding to ARE of its downstream genes[33]. Among these, HO-1 has most abundant sites for ARE on its promoter region[13]. Suppression on HO-1 could promote ferroptosis via its multiple functions: (i) alleviate ROS formation via suppression on its anti-oxidant activity[34]; (ii) Stabilize nuclear Nrf2 via its

nuclear translocation in enzymatically inactive form[35]; (iii) decrease the capture on redox-active to increase LIP[36]. Thus, inactivation Nrf2/HO-1 axis could contribute to the ferroptosis promotion. Consistent with this notion, the application of gingketin in DDP-treated cells decreased Nrf2 expression, attenuated DDP-induced increase on binding of Nrf2 to HO-1 promote region, as well as the expression and nuclear translocation of HO-1. These phenomena indicated ginkgetin attenuated DDP-induced Nrf2/HO-1 activation, which could in turn increase LIP and ROS formation, further promote ferroptosis, and the consequent redox homeostasis disruption in ginkgetin + DDP treated NSCLC cells.

LIP consists of Free ferrous iron (Fe^{2+}) in the cytosol. The promoted LIP level discovered here could contribute to elevated Fe^{2+}, promote ROS formation[11]. Excess ROS generated by iron might promote redox homeostasis resetting to the development of a tumor. ROS plays a central role in DDP-induced anti-cancer effect. Cancer cells can evade DDP-induced ROS formation via redox homeostasis resetting. To this regard, persistent ROS elevation contributes to an adaptive response of cancer cells, leading them to survive under high ROS level. Here, we found DDP sharply increased ARE-mediated activity, i.e. binding of Nrf2 onto HO-1 promoter. Supporting this notion, the ARE-mediated activity was much robust in DDP-resistance cells (Fig. S7). In addition, GSH/GSSG, a system also contribute to the antioxidant, was upregulated after DDP application. These lines of evidence indicated that DDP could trigger a resetting on redox homeostasis, as to cope with increased ROS level in A549 cells. Here, the DDP-induced redox homeostasis resetting could be disrupted by ginkgetin, which was demonstrated by the sharply promoted ROS formation, Nrf2/HO-1 inactivation and GSH/GSSG downregulation in DDP-treated NSCLC cells.

When the ROS level over threshold, MMP loss could be triggered via opening permeability of mitochondria [37]. This further causes cytochrome c release and caspase-9 activation[38], which subsequently accelerate the activation of caspase-3 and 7, finally triggering apoptosis[39]. Consistent with this notion, increases of MMP loss, activated caspase-9,7,3 and apoptosis rate were found in ginkgetin + DDP-treated NSCLC cells. This phenomenon indicated that apoptosis was also promoted.

However, blocking Nrf2, ROS formation and apoptosis did not compromise gingketin-induced promotion on DDP-induced cytotoxicity. While pharmaceutical and genetic suppression on ferroptosis compromised ginkgetin induced promotion on cytotoxicity. In addition, ginkgetin induced promotion on ROS formation, MMP loss and apoptosis in DDP-treated NSCLC cells were all reversed by ferroptosis inhibition. These phenomena indicated the crucial role of ferroptosis in ginkgetin + DDP induced anticancer effect. Ferroptosis induction might at early stage in ginkgetin + DDP induced cytotoxicity. The application of ginkgetin on DDP-treated NSCLC cells firstly triggered ferroptosis cascade, i.e. SLC7A11 and GPX4 suppression, leading to mitigation on antioxidant activity of GSH/GSSG and Nrf2/HO-1 axis, which contribute to redox homeostasis disruption, finally enhanced DDP-induced cell death (Fig. 8).

Conclusions

In short, ferroptosis contributes to the increased cytotoxicity induced by ginkgetin in DDP-treated EGFR wild type NSCLC. Several studies reported the benefits for combination of ferroptosis and apoptosis

inducers on cancer treatment. This phenomenon was confirmed by our study that ginkgetin-induced ferroptosis and DDP-induced apoptosis were both amplified under the drug combination. Notwithstanding, how ferroptosis promote apoptosis, what contributes to the downregulation of SLC7A11, GPX4, and how ferroptosis promotion downregulate Nrf2/HO-1 in ginkgetin + DDP treated cells are needed to be further elucidated. As the overall survival rate of NSCLC is still needed to be improved, the current discovery could be a promising strategy for NSCLC treatment.

Abbreviations

CA-AM, Calcein-acetoxymethyl ester; DCFH-DA, 2',7'-dichlorofluorescin diacetate; DDP, cisplatin; DFO, desferoxamine; DMF, fumarate; GPX4, glutathione peroxidase 4; GSH, glutathione; GSSG, glutathione; glutathione disulfide; JC-1, 5,5',6,6'-tetrachloro-1,1',3,3'-tetraethyl-imidacarbocyanine iodide; MMP, mitochondrial membrane potential; NAC, N-acetylcysteine; NSCLC, non-small cell lung cancer; Nrf2, nuclear factor erythroid 2
related factor 2; SFN, sulforaphane; SLC40A1, Solute Carrier Family 40 Member 1; SLC7A11, solute carrier family 7 member 11.

Declarations

Acknowledgements

Not applicable

Authors' contributions

J.S.L. and T.X. conceived and designed the experiments. J.S.L. and K.W.T. wrote the main text. L.P.Z performed cytotoxicity assay, ferroptosis and redox balance evaluation. J.T.X fit the dose-response surface. X.Y.C conducted the translocation analysis, apoptosis analysis. C.S.W. perform the animal study. C.Y.T analyzed the data. *Z.H.H supervised the study and revised the manuscript.*

Funding

This work is supported by the Key projects of National Natural Science Foundation of China [81730108]; the Key Project of Zhejiang province Ministry of Science and Technology [2015C03055]; The Shenzhen Science and Technology Innovation Committee [ZDSYS201707281432317; JCYJ20170413173747440; JCYJ20180306174903174]; the Zhongshan Municipal Bureau of Science and Technology [ZSST20SC03]; the Hong Kong Innovation Technology Fund [UIM/340, UIM/385, ITS/500/18FP; TCPD/17-9;

HMRF18SC06]; The Natural Science Foundation of Zhejiang Province [LY20H280011]; and the Medical Health Science and Technology Project of Zhejiang Provincial Health Commission [2020367195].

Availability of data and materials

The datasets used and analysed during the current study are available from the corresponding author on reasonable request.

Ethics approval and consent to participate

Not applicable

Consent for publication

Not applicable

Competing interests

The authors declare that they have no competing interests

References

1. Cao M, Chen W. Epidemiology of lung cancer in China. Thorac Cancer. 2019;10:3–7.
2. Yang D, Liu Y, Bai C, Wang X, Powell CA. Epidemiology of lung cancer and lung cancer screening programs in China and the United States. Cancer Lett. 2020;468:82–7.
3. Vasconcellos VF, Marta GN, da Silva EM, Gois AF, de Castria TB, Riera R. Cisplatin versus carboplatin in combination with third-generation drugs for advanced non-small cell lung cancer. Cochrane Database Syst Rev. 2020;1:CD009256.
4. Sun CY, Zhang QY, Zheng GJ, Feng B. Phytochemicals: current strategy to sensitize cancer cells to cisplatin. Biomed Pharmacother. 2019;110:518–27.
5. Hirschhorn T, Stockwell BR. The development of the concept of ferroptosis. Free Radic Biol Med. 2019;133:130–43.
6. Guo J, Xu B, Han Q, Zhou H, Xia Y, Gong C, et al. Ferroptosis: a novel anti-tumor action for cisplatin. Cancer Res Treat. 2018;50:445–60.

7. Roh JL, Kim EH, Jang HJ, Park JY, Shin D. Induction of ferroptotic cell death for overcoming cisplatin resistance of head and neck cancer. Cancer Lett. 2016;381:96–103.
8. Sato M, Kusumi R, Hamashima S, Kobayashi S, Sasaki S, Komiyama Y, et al. The ferroptosis inducer erastin irreversibly inhibits system Xc^- and synergizes with cisplatin to increase cisplatin's cytotoxicity in cancer cells. Sci Rep. 2018;8:968.
9. Koppula P, Zhang Y, Zhuang L, Gan B. Amino acid transporter SLC7A11/xCT at the crossroads of regulating redox homeostasis and nutrient dependence of cancer. Cancer Commun (Lond). 2018;38:12.
10. Forcina GC, Dixon SJ. GPX4 at the crossroads of lipid homeostasis and ferroptosis. Proteomics. 2019;19:e1800311.
11. Mou Y, Wang J, Wu J, He D, Zhang C, Duan C, et al. Ferroptosis, a new form of cell death: opportunities and challenges in cancer. J Hematol Oncol. 2019;12:34.
12. Yu H, Guo P, Xie X, Wang Y, Chen G. Ferroptosis, a new form of cell death, and its relationships with tumourous diseased. J cell Mol Med. 2017;21:648–57.
13. Loboda A, Damulewicz M, Pyza E, Jozkowicz A, Dulak J. Role of Nrf2/HO-1 system in development, oxidative stress response and diseases: an evolutionarily conserved mechanism. Cell Mol Life Sci. 2016;73:3221–47.
14. Hu WH, Chan GK, Duan R, Wang HY, Kong XP, Dong TT, et al. Synergy of ginkgetin and resveratrol in suppressing VEGF-induced angiogenesis: a therapy in treating colorectal cancer. Cancers (Basel). 2019;11:1828.
15. Lou JS, Bi WC, Chan GKL, Jin Y, Wong CW, Zhou ZY, et al. Ginkgetin induces autophagic cell death through p62/SQSTM1-mediated autolysosome formation and redox setting in non-small cell lung cancer. Oncotarget. 2017;8:93131–48.
16. Cao J, Tong C, Liu Y, Wang J, Ni X, Xiong MM. Ginkgetin inhibits growth of breast carcinoma via regulating MAPKs pathway. Biomed Pharmacother. 2017;96:450–8.
17. Gao M, Monian P, Pan Q, Zhang W, Xiang J, Jiang X. Ferroptosis is an autophagic cell death process. Cell Res. 2016;26:1021–32.
18. Park E, Chung SW. ROS-mediated autophagy increases intracellular iron levels and ferroptosis by ferritin and transferrin receptor regulation. Cell Death Dis. 2019;10:822.
19. Lou JS, Xia YT, Wang HY, Kong XP, Yao P, Dong TTX, et al. The WT1/MVP-mediated stabilization on mTOR/AKT axis enhances the effects of cisplatin in non-small cell lung cancer by a reformulated Yu Ping Feng San herbal preparation. Front Pharmacol. 2018;9:853.
20. Lou JS, Yan L, Bi CW, Chan GK, Wu QY, Liu YL, et al. Yu Ping Feng San reverses cisplatin-induced multi-drug resistance in lung cancer cells via regulating drug transporters and p62/TRAF6 signalling. Sci Rep. 2016;6:31926.
21. Lei P, Bai T, Sun Y. Mechanisms of ferroptosis and relations with regulated cell death: a review. Front Physiol. 2019;10:139.

22. Ortega Ferrusola C, González Fernández L, Morrell JM, Salazar Sandoval C, Macías García B, Rodríguez-Martinez H, et al. Lipid peroxidation, assessed with BODIPY-C11, increases after cryopreservation of stallionspermatozoa cryopreservation of stallionspermatozoa, is stallion-dependent and is related to apoptotic-like changes. Reproduction. 2009;138:55–63.
23. Ka C, Guellec J, Pepermans X, Kannengiesser C, Ged C, Wuyts W, et al. The SLC40A1 R178Q mutation is a recurrent cause of hemochromatosis and is associated with a novel pathogenic mechanism. Haematologica. 2018;103:1796–805.
24. Stockwell BR, Friedmann Angeli JP, Bayir H, Bush AI, Conrad M, Dixon SJ, et al. Ferroptosis: a regulated cell death nexus linking metabolism, redox biology, and disease. Cell. 2017;171:273–85.
25. Dodson M, Castro-Portuguez R, Zhang DD. NRF2 plays a critical role in mitigating lipid peroxidation and ferroptosis. Redox Biol. 2019;23:101107.
26. Panieri E, Saso L. Potential applications of NRF2 inhibitors in cancer therapy. Oxid Med Cell Longev. 2019;2019:8592348.
27. Vanella L, Barbagallo I, Tibullo D, Forte S, Zappalà A, Li Volti G. The non-canonical functions of the heme oxygenases. Oncotarget. 2016;7:69075–86.
28. Dixon SJ, Lemberg KM, Lamprecht MR, Skouta R, Zaitsev EM, Gleason CE, et al. Ferroptosis: an iron-dependent form of nonapoptotic cell death. Cell. 2012;149:1060–72.
29. Maiorino M, Conrad M, Ursini F. GPX4, lipid peroxidation, and cell death: discoveries rediscoveries, and open issues. Antioxid Redox Signal. 2018;29:61–74.
30. Wu Z, Geng Y, Lu X, Shi Y, Wu G, Zhang M, et al. Chaperone-mediated autophagy is involved in the execution of ferroptosis. Proc Natl Acad Sci USA. 2019;116:2996–3005.
31. Yu X, Long YC. Crosstalk between cystine and glutathione is critical for the regulation of amino acid signaling pathways and ferroptosis. Sci Rep. 2016;6:30033.
32. Fujii J, Homma T, Kobayashi S. Ferroptosis caused by cysteine insufficiency and oxidative insult. Free Radic Res. 2019;1–12.
33. Itoh K, Mimura J, Yamamoto M. Discovery of the negative regulator of Nrf2, Keap1: a historical overview. Antioxid Redox Signal. 2010;13:1665–78.
34. Furfaro AL, Traverso N, Domenicotti C, Piras S, Moretta L, Marinari UM, et al. The Nrf2/HO-1 axis in cancer cell growth and chemoresistance. Oxid Med Cell Longev. 2016;2016:1958174.
35. Biswas C. Shah N, Muthu M. La P, Fernando AP. Sengupta S. et al. Nuclear heme oxygenase-1 (HO-1) modulates subcellular distribution and activation of Nrf2, impacting metabolic and anti-oxidant defenses. J Biol Chem. 2014;289:26882-94.
36. Mai TT, Hamaï A, Hienzsch A, Cañeque T, Müller S, Wicinski J, et al. Salinomycin kills cancer stem cells by sequestering iron in lysosomes. Nat Chem. 2017;9:1025–33.
37. Zhou L, Jiang L, Xu M, Liu Q, Gao N, Li P, et al. Miltirone exhibits antileukemic activity by ROS-mediated endoplasmic reticulum stress and mitochondrial dysfunction pathways. Sci Rep. 2016;6:20585.

38. Kadenbach B, Arnold S, Lee I, Hüttemann M. The possible role of cytochrome c oxidase in stress-induced apoptosis and degenerative diseases. Biochim Biophys Acta. 2004;1655:400–8.
39. McIlwain DR, Berger T, Mak TW. Caspase functions in cell death and disease. Cold Spring Harb Perspect Biol. 2015;7(4):a026716.

Figures

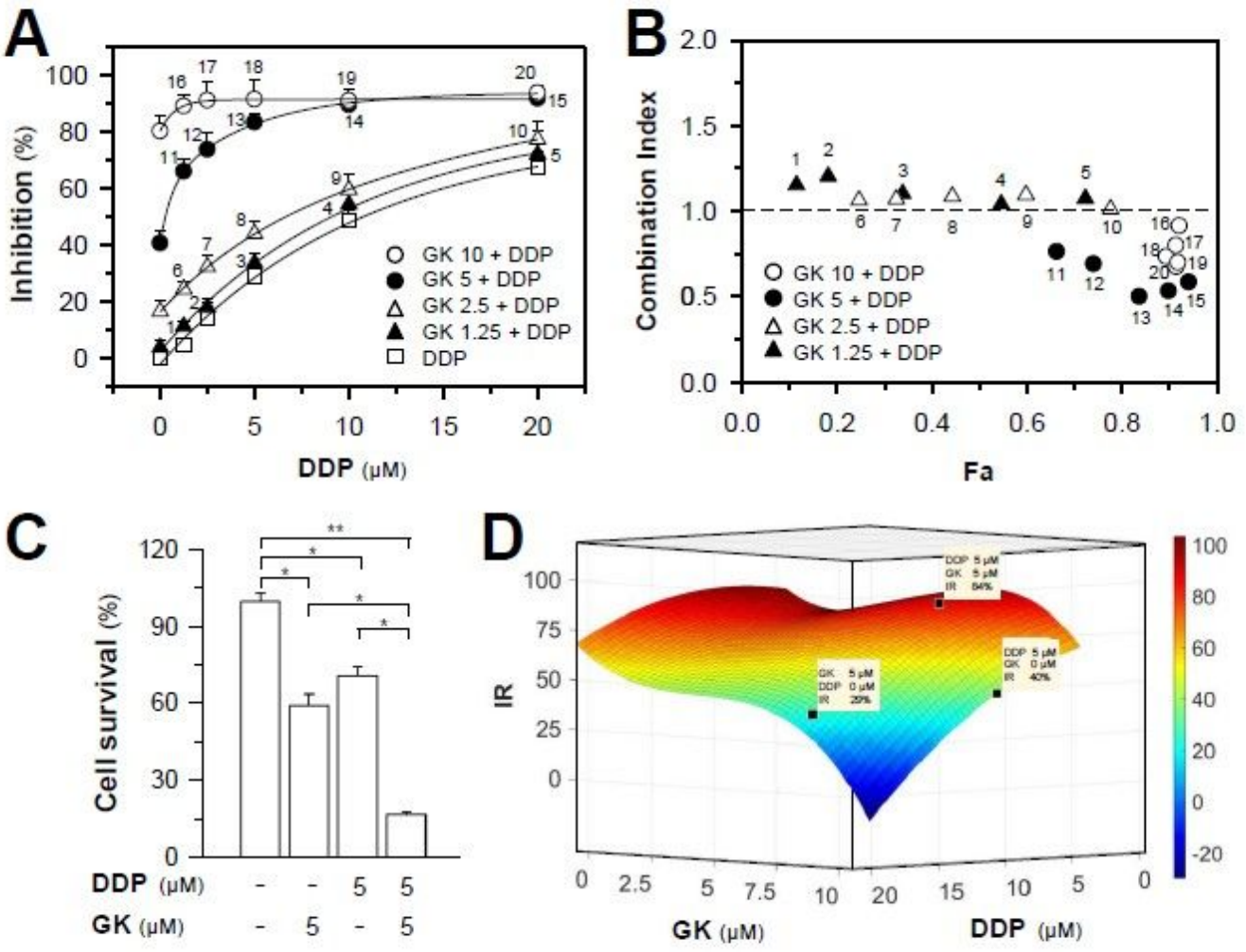

Figure 1

Synergistic effect of ginkgetin and DDP in A549 cells. (A): Cells were seeded in 96-well plates (3 X 103 cells/well). Different concentrations of DDP (1.25, 2.5, 5, 10, 20 μM) with or without various concentration

of ginkgetin (1.25, 2.5, 5, 10 μM) were added for 48 hours. Values are in percentage of cell growth inhibition. (B): Combination Index (CI) of 20 combinations were calculated using CompuSyn software. CI values <1, =1 and >1 indicate synergism, additive effect and antagonism, respectively. (C): The IC50 value of ginkgetin (5 μM), DDP (5 μM), and ginkgetin + DDP (5 μM+5 μM) on A549 cells. (D): Dose–response surface was fitted by MATLAB to determine interaction between ginkgetin and DDP. Each point represents the mean ± SEM, n = 3. *p < 0.05, **p < 0.01. GK: ginkgetin.

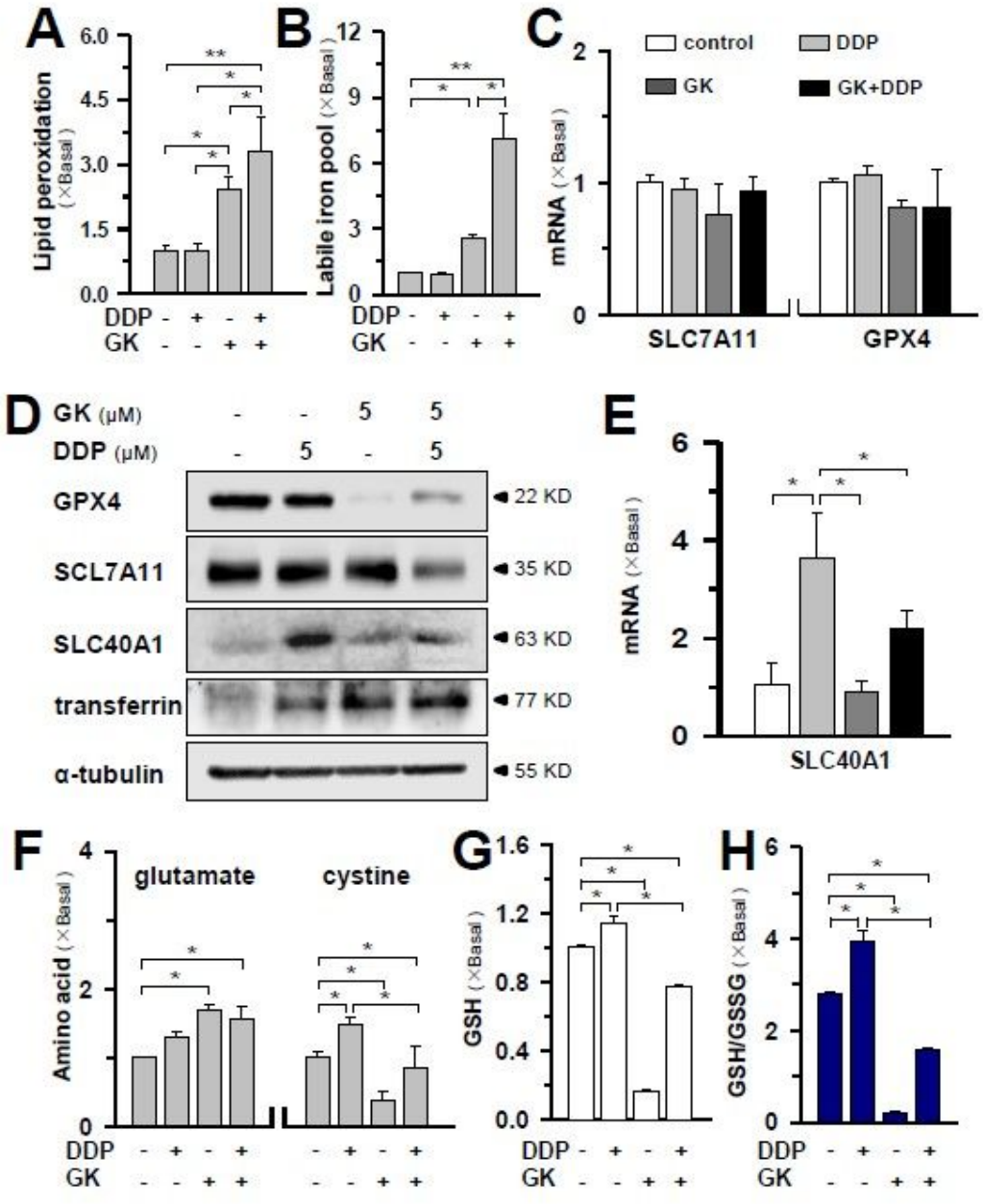

Figure 2

Ginkgetin induces ferroptosis in DDP-treated A549 cells (A): Cultured A549 cells were treated with ginkgetin (5 μM), DDP (5 μM), and ginkgetin + DDP (5 μM+5 μM) for 48 hours. Cells were stained with BODIPY™ 581/591 C11 (10 μM) for 30 min, the level of lipid peroxidation was detected by flow cytometry. (B): Cells were treated as in (A), then CA-AM was added to cells at the final concentration of 0.25 μM, followed by adding iron chelator deferiprone (100 μM) for 1 hour or left untreated. The mean fluorescence was detected fluorescence microplate reader (Exc=488 nm, Em=525 nm). The amount of LIP was reflected via difference on mean fluorescence of each sample with or without deferiprone. (C): Cells were treated as in (A), The mRNA expression of SLC7A11, GPX4 were detected by qPCR. (D): Cells were treated as in (A), the protein expression of GPX4, SLC7A11, SLC40A1 and transferrin were detected by western blot. (E) Cells were treated as in (A), The mRNA expression of SLC40A1 were detected by qPCR. (F): Cells were treated as in (A), then collect and lysed, the amount of glutamate and cystine were detected by LC-MS. (G & H): Cells were treated as in (A), the levels of GSH and GSSG were measured by GSH and GSSG Assay kit. Values are in fold of change (X Basal) to control (no drug treatment). Each point represents the mean ± SEM, n = 3. *$p < 0.05$, **$p < 0.01$. GK: ginkgetin.

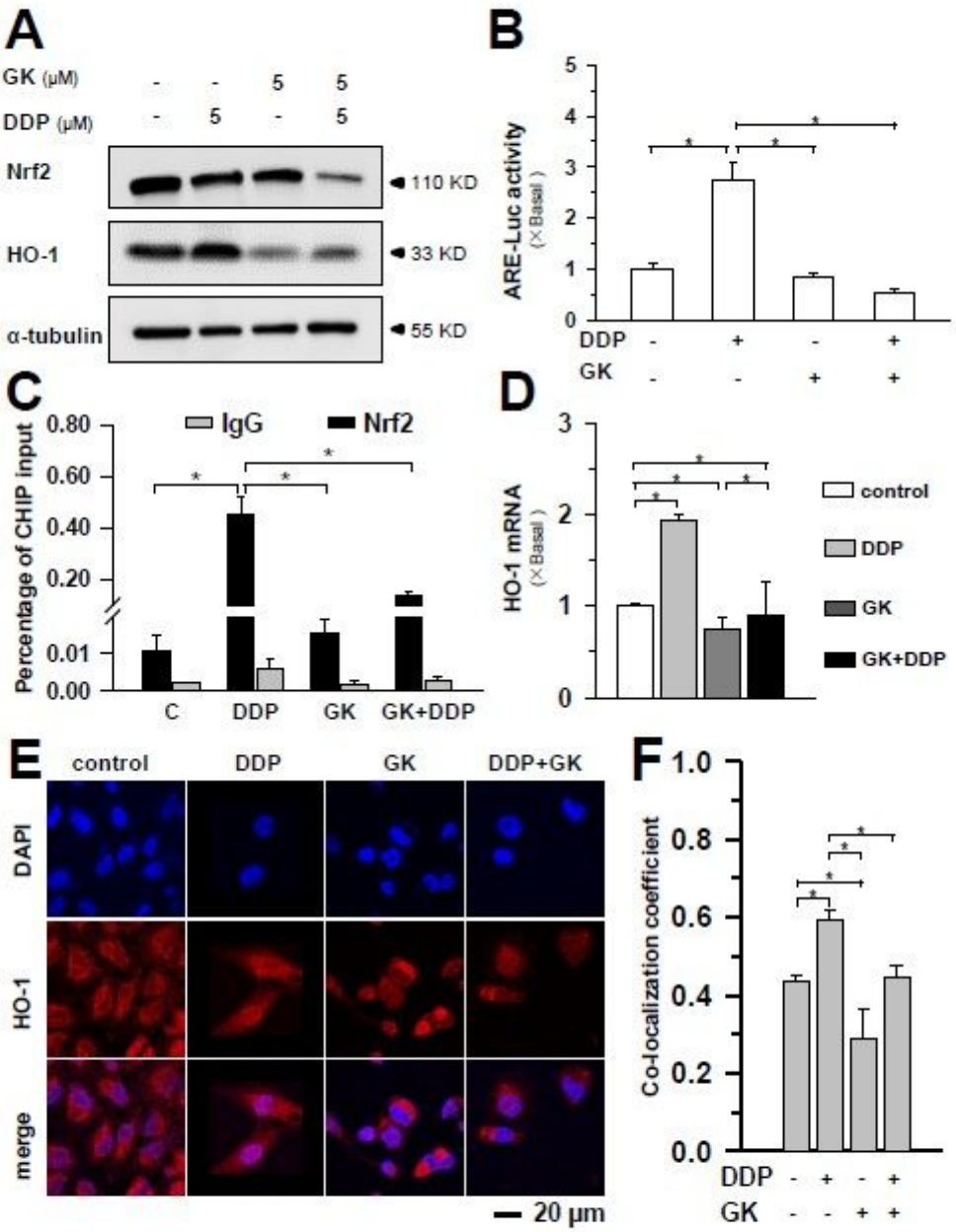

Figure 3

Ginkgetin reverses DDP-induced elevation on Nrf2/HO-1 antioxidant system. (A): Culture A549 cells were treated with ginkgetin (5 μM), DDP (5 μM), and ginkgetin + DDP (5 μM+5 μM) for 48 hours. The protein expressions of Nrf2 and HO-1 were analyzed by western blot. (B): A549 cells were seeded in 6-well plates, pARE-Luc was transfected for 4 hours, then drug treatments were same as in (A), pARE-Luc activity was detected by luciferase assay. (C): Drug treatment was applied as in (A), chromatin was sheared and

incubated with either anti-Nrf2 antibody, IgG, or H3 antibody. Purified DNA was analyzed by quantitative real-time qPCR. The expression of each sample was presented as a percent of the total input chromatin. (D): Cells were treated as in (A), The amount of mRNA encoding HO-1 was determined by real-time PCR. Values are in fold of change (X Basal) to control (no drug treatment). (E): The localization of HO-1 (red fluorescence) in nuclei (blue fluorescence) was observed by immunofluorescence. Bar = 20 μm. (F): Co-localization coefficients were calculated by the co-localizing pixel for HO-1 relative to the total number of pixels for the nuclei using Olympus Fluoview FV31S-DT Software. Each point represents the mean ± SEM, n = 3. *p < 0.05. GK: ginkgetin.

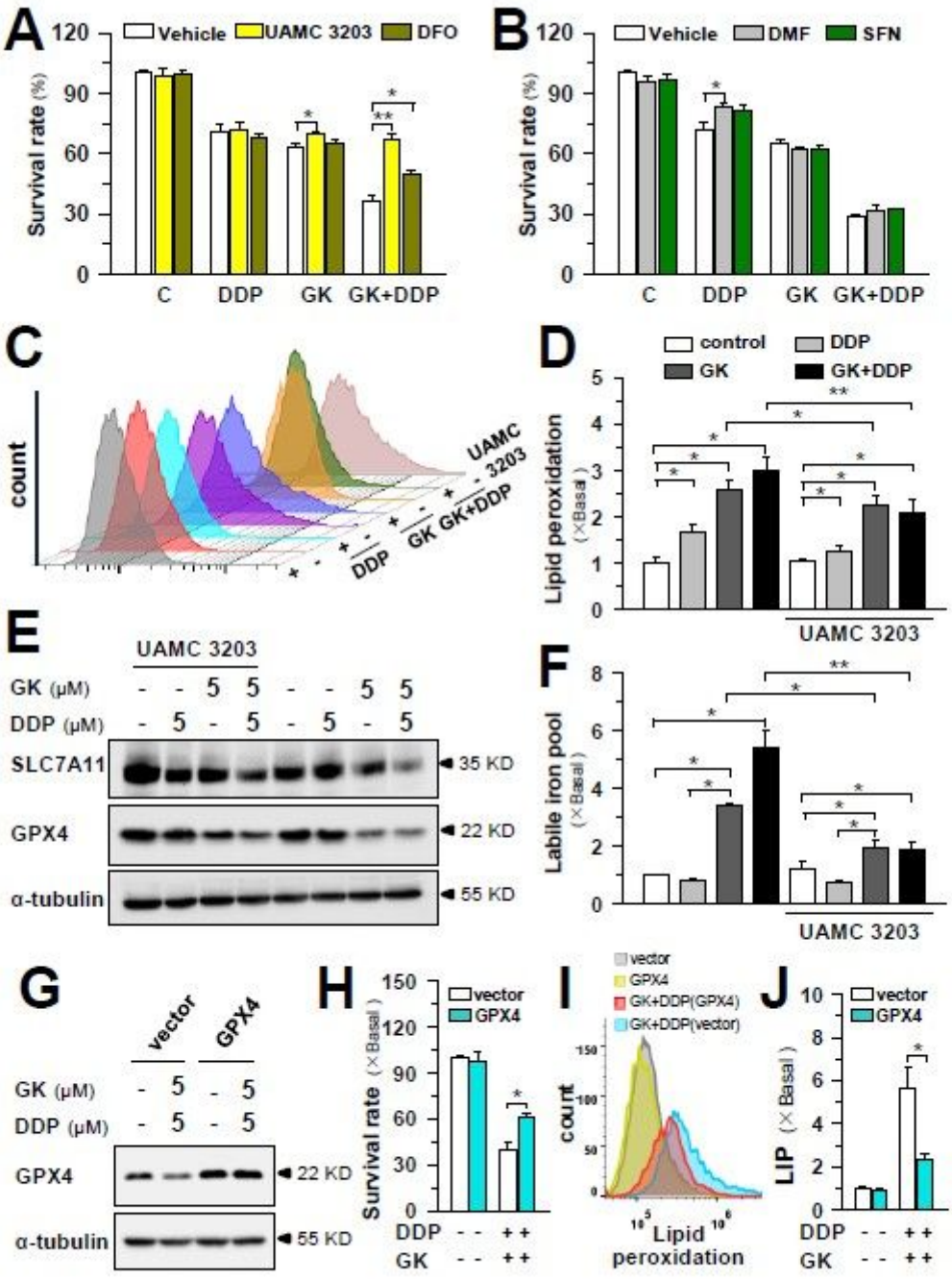

Figure 4

Blocking ferroptosis reversed ginkgetin+DDP induced cytotoxicity (A&B): Cultured A549 cells were seeded in 96-well plate, ginkgetin (5 μM), DDP (5 μM), and ginkgetin + DDP (5 μM+5 μM). A: with or without UAMC 3203 (25 nM), or DFO (200 μM); B: with or without DMF (100 nM), or SFN (10 μM) were added for 48 hours. Cell viability was detected by MTT assay. Values are in percentage of cell growth inhibition. (C): Cells were treated with ginkgetin (5 μM), DDP (5 μM), and ginkgetin + DDP (5 μM+5 μM) with or without UAMC 3203 (25 nM) for 48 hours, and stained with BODIPY™ 581/591 C11 (10 μM) for 30 min. The level of lipid peroxidation was detected by flow cytometry. (D): Quantitation on mean fluorescence was calibrated from (C). (E): Cells were treated as in (C), the protein expressions of SLC7A11, GPX4 were detected by western blot. (F): Cells were treated as in (C), then CA-AM was added to cells at the final concentration of 0.25 μM, followed by adding iron chelator deferiprone (100 μM) for 1 hour or left untreated. The mean fluorescence was detected fluorescence microplate reader (Exc=488 nm, Em=525 nm). The amount of LIP was reflected via difference on mean fluorescence of each sample with or without deferiprone. (G): Cultured A549 cells were transfected with either vector and pNIC28-Bsa4-GPX4 plasmids, then treated with or without ginkgetin + DDP (5 μM+5 μM) for 48 h, the expression of GPX4 were detected by western blot. (H): Cells were transfected and treated as in (G), MTT assay were conducted as in Fig.1A. (I): Cells were transfected and treated as in (G), lipid peroxidation was detected as in (C). (J): Cells were transfected and treated as in (G), LIP assay was conducted as in (F). Each point represents the mean ± SEM, n = 3. *$p < 0.05$, **$p < 0.01$. C: control; GK: ginkgetin.

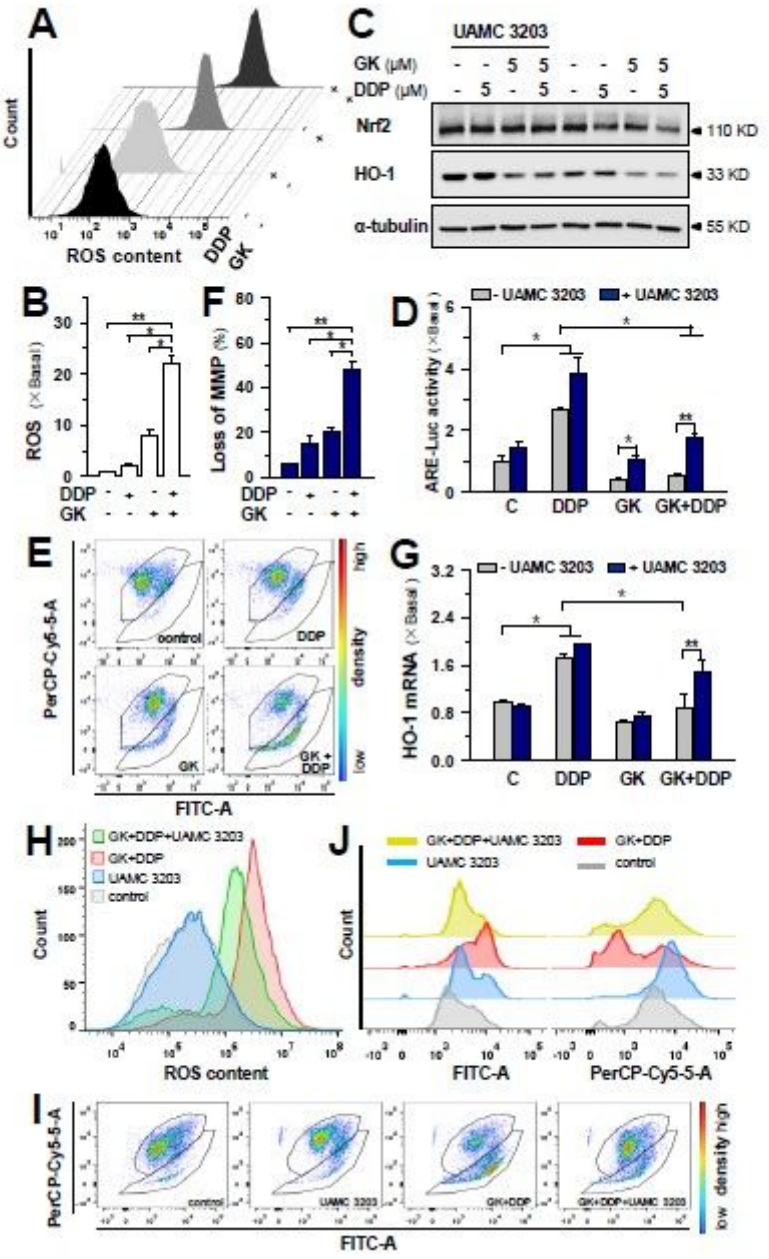

Figure 5

Ferroptosis inhibition mitigates ginkgetin induced Nrf2/HO-1 inactivation, ROS increase and MMP loss in DDP-treated A549 cells. (A): Cultured A549 cells were treated with ginkgetin (5 μM), DDP (5 μM), and ginkgetin + DDP (5 μM+5 μM) for 48 h. Cells were stained with DCFH-DA (15 μM) for 30 min. The ROS formation were detected by flow cytometry. (B): Quantitation on mean fluorescence was calibrated from (A). (C): Cells were treated with ginkgetin (5 μM), DDP (5 μM), and ginkgetin + DDP (5 μM+5 μM) with or without UAMC 3203 (25 nM) for 48 hours, the protein expressions of Nrf2, HO-1 were detected by western blot. (D): In pARE-Luc transfected cells for 4 hours, the cells were treated as in (C). pARE-Luc activity was detected by luciferase assay. (E): Cells were treated as in (A) and stained with JC-1 (2 μM) for 30 min. MMP was detected by flow cytometry. (F): The MMP loss was calibrated from (C). values are in fold of

change (X Basal) to control (no drug treatment). (G): Cells were treated as in (C), the mRNA level of HO-1 was detected by qPCR. Values are in fold of change (X Basal) to control (no drug treatment). (H): Cells were treated with ginkgetin + DDP (5 μM+5 μM) in the presence and absence of UAMC 3203 (25 nM), then stained with DCFH-DA (15 μM) for 30 min. The ROS formation were detected by flow cytometry. (I): Cells were treated as in (H) and stained with JC-1 (2 μM) for 30 min. MMP was detected by flow cytometry. (J): The histogram overlay in half offset format to reveal the mean fluorescence of FTIC and PerCP-Cy5-5 channel calibrate from (I). Each point represents the mean ± SEM, n = 3. *p < 0.05, **p < 0.01. GK: ginkgetin.

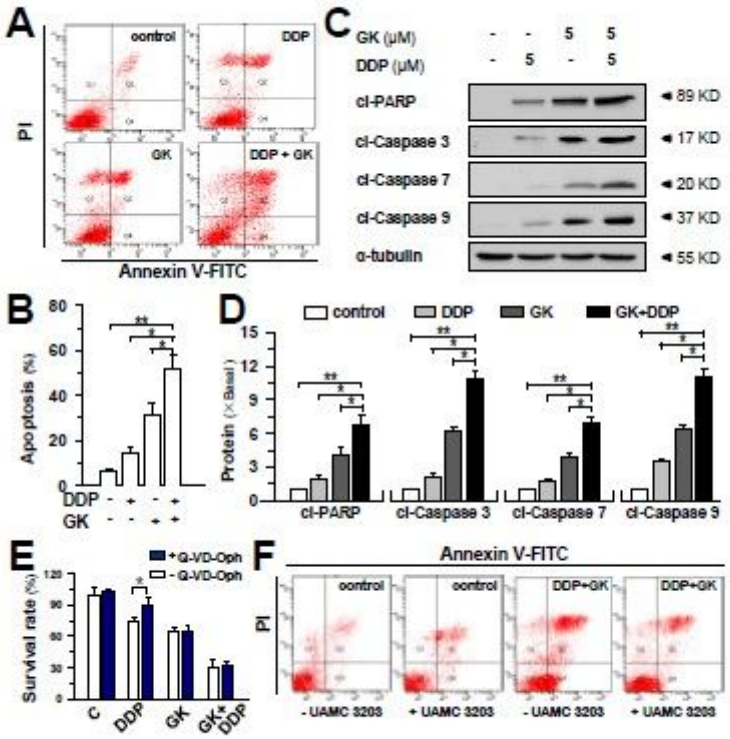

Figure 6

Ginkgetin enhances DDP-induced apoptosis in A549 cells and alleviate by ferroptosis inhibition. (A): Cultured A549 cells were treated with ginkgetin (5 μM), DDP (5 μM), and ginkgetin +DDP (5 μM+5 μM) for 48 hours. Cell were stained with Annexin V and PI and analyzed by flow cytometry. Q2 quadrant in the top right represents late apoptotic cells, Q3 in the left bottom quadrant represents viable cell population, Q4 in the right bottom represents early apoptotic cells. (B): Determination of apoptotic rates, as calibrated from (A). Values are in percentage of apoptotic cell number. (C): Western blot analyses of cleaved-PARP, cleaved caspase-3, -7, -9. Expression of β-tubulin served as a control. (D): Semi-quantitation of cleaved-PARP, cleaved caspase-3, -7, -9, as calibrated from (C). Values are in fold of change (X Basal) to control (no drug treatment). (E): ginkgetin (5 μM), DDP (5 μM), and ginkgetin + DDP (5 μM+5 μM), with or without Q-VD-Oph (20 μM) were added. Cell viability was detected by MTT assay. Values are in percentage of cell

growth inhibition. (F): Cells were treated with ginkgetin + DDP (5 μM+5 μM) in the presence and absence of UAMC 3203 (25 nM), apoptosis analysis was conducted as in (A). Each point represents the mean ± SEM, n = 3. *p < 0.05, **p < 0.01. GK: ginkgetin.

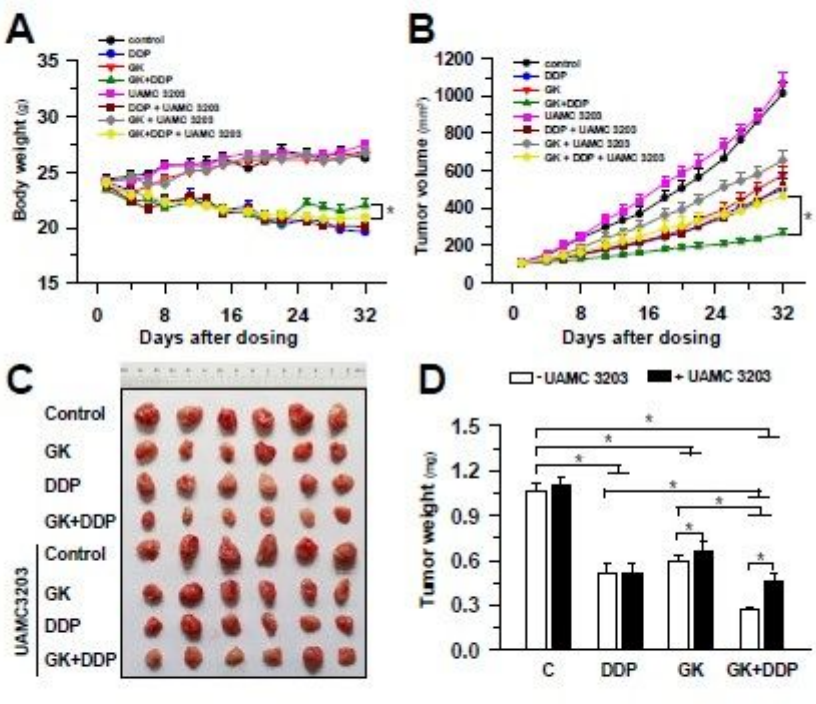

Figure 7

The enhanced anticancer effect of DDP induced by ginkgetin was reversed by UAMC 3203 in NSCLC xenograft nude mice model. A549 lung cancer cells were subcutaneously implanted in the flank of nude mice. The tumors were allowed to grow at ~100 mm3 and randomly divided into 8 groups: control, ginkgetin, DDP, ginkgetin + DDP, UAMC3203, ginkgetin + UAMC 3203, DDP + UAMC3203, ginkgetin + DDP + UAMC 3203. Thereafter, DDP (3 mg/kg), ginkgetin (30 mg/kg), ginkgetin (30 mg/kg) +DDP (3 mg/kg) in the absence, or presence of UAMC 3203 (10 mg/kg), were administered. (A): The body weight was checked 2-3 times per week over a period of 32 days. (B): The mean tumor volume in each group after drug treatment. (C): Tumors excised out of the mice at day 32. (D): Mean tumor weight in each group at the end of treatment. Data represents Mean ± SEM, n = 6. *p <0.05. C: control; GK: ginkgetin.

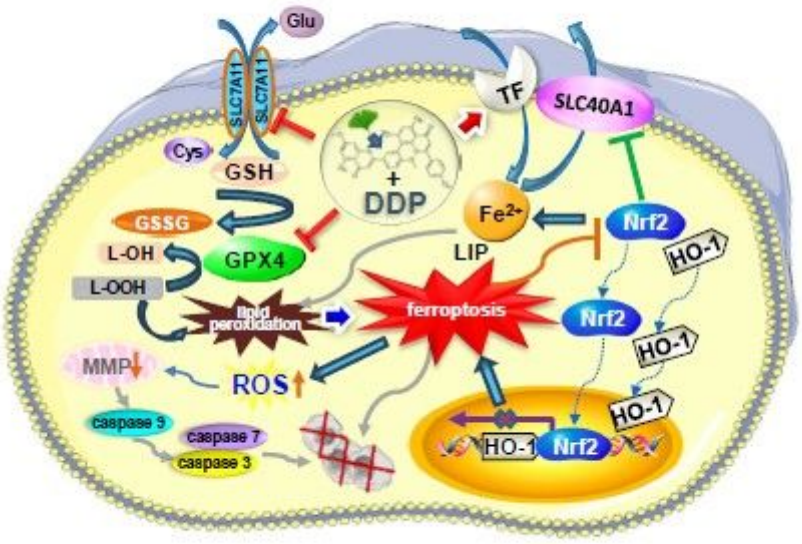

Figure 8

The schematic diagram on the mechanism of ginkgetin induced promotion on DDP-induced anticancer effect via ferroptosis. Ginkgetin + DDP induced ferroptosis cell death could be induced by: i) suppression on SLC7A11, GPX4, leading to the disruption on GSH-mediated redox balance to promote lipid peroxidation. (ii) regulation on iron transporters transferrin and SLC40A1, which promote the intracellular iron concentration and lipid peroxidation. The increased ferroptosis level could further disrupt the redox homeostasis via Nrf2/HO-1 inactivation and ROS enhancement, which further promoted DDP-induced cell death, including apoptosis. The inactivation of Nrf2/HO-1 could suppress on SLC40A1 to enhance iron, which could in turn promoted ferroptosis in ginkgetin + DDP treated NSCLC cells.

Supplementary Files

This is a list of supplementary files associated with this preprint. Click to download.

- 35Supplementarydata.docx